

Potential vibrational modes tied to diffuse interstellar bands

Daniel Majaess^{1,2}  Halis Seuret,^{1,2} Tina A. Harriott^{1,3}  Cercis Morera-Boado^{1,4}  Ailish D. Sullivan,¹ Lou Massa⁵ and Chérif F. Matta^{1,6,7,8}

¹Department of Chemistry and Physics, Mount Saint Vincent University, Halifax, Nova Scotia, B3M2J6, Canada

²Centro de Investigaciones Químicas, IICBA, Universidad Autónoma del Estado de Morelos, Cuernavaca, 62209, Morelos, Mexico

³Department of Mathematics and Statistics, Mount Saint Vincent University, Halifax, Nova Scotia, B3M2J6, Canada

⁴IXM-Cátedra Conacyt-Centro de Investigaciones Químicas, IICBA, Universidad Autónoma del Estado de Morelos, Cuernavaca, 62209, Morelos, Mexico

⁵Hunter College & the PhD Program of the Graduate Center, City University of New York, New York 10016, USA

⁶Department of Chemistry, Saint Mary's University, Halifax, Nova Scotia, B3H3C3, Canada

⁷Département de Chimie, Université Laval, Québec, G1V0A6, Canada

⁸Department of Chemistry, Dalhousie University, Halifax, Nova Scotia, B3H4J3, Canada

Accepted 2025 April 17. Received 2025 April 6; in original form 2025 January 2

Downloaded from https://academic.oup.com/mnras/article/539/4/3489/8123622 by guest on 14 May 2025

ABSTRACT

Potential vibrational modes associated with diffuse interstellar bands (DIBs) could be discerned by examining energy differences between correlated DIBs. Consequently, $\approx 10^3$ higher correlated DIB pairs ($r - \sigma_r \geq 0.8, \geq 12$ sightlines) were extracted from the Apache Point Observatory DIB catalogue, and their energy spacings computed. In this first macro exploratory step, a histogram possibly reveals chemical bond signatures of $C\equiv C$, $C\equiv N$, $S-H$, $C-O$, $C=O$, $Si-H$, $N-H$, $C-H$ (aliphatic), $C\cdots C$ (in-ring), and aromatics ($C-H$ stretch, $C\cdots C$ in-ring, oop $C-H$ bending, overtones and combinations). Continued research is required to (in)validate the histogram approach, mitigate noise, scrutinize maxima, break degeneracies, and converge upon an optimal framework.

Key words: ISM: molecules.

1 INTRODUCTION

Heger (1922) observed that absorption lines at 5780 and 5797 Å were superposed upon the spectra of binary stars, granted they lacked the requisite oscillatory Doppler shifting. The molecular source(s) behind those lines are mainly within interstellar clouds along the sightline (see also Hartmann 1904, regarding interstellar calcium). A century later several hundred diffuse interstellar bands (DIBs) are known (e.g. Bondar 2012; Fan et al. 2019). PAHs remain a leading hypothesis as a principal carrier (e.g. Bondar 2020), and for several DIBs C_{60}^+ is debated (e.g. Campbell et al. 2015; Galazutdinov et al. 2017, 2021; Schlarbmann et al. 2021; Nie, Xiang & Li 2022; Majaess et al. 2025). Indeed, heterofullerenes and (endo/exo)hedral inclusions are likewise being explored as DIB carriers (e.g. Kroto 1987; Omont 2016).

Here, the objective is to explore whether vibrational transitions may be identified by delineating energy differences between correlated DIB pairs (e.g. Jenniskens & Desert 1993; Moutou et al. 1999; Bondar 2020). For example, Jenniskens & Desert (1993) suggested the energy separation between DIBs 5797 and 6269 Å could be indicative of a PAH $C=C$ vibration (7.7 μm). Moutou et al. (1999) underscored that the gap between the correlated 6196 and 6614 Å DIBs is tied to an aromatic mode (9.8 μm). Bondar (2020, their table 4) relays that the energy offset between DIBs 5545 and 6614 Å may be linked to PAH or aliphatic $C-H$ (3.3 μm). DIBs associated with

a given molecule may represent a vibronic progression (e.g. McCall et al. 2010, and discussion therein).

2 ANALYSIS

The Fan et al. (2019) APO catalogue was examined, and the analysis was subsequently limited to DIB pairs exhibiting higher Pearson correlated equivalent widths ($r - \sigma_r \geq 0.8, EW/\sigma_{EW} \geq 5$), possessing ≥ 12 sightlines, and whose energy difference falls within $500-4000\text{ cm}^{-1}$. The Pearson correlation, equivalent width, and their uncertainties are described by r , σ_r , EW , and σ_{EW} . The sightline to VI Cyg 12 was excluded owing to its circumstellar shell and color-excess beyond the field (e.g. Maryeva et al. 2016; Xing et al. 2024).

The final sample hosts $\approx 10^3$ DIB pairs. Wavenumbers linked to the energy spacing between DIB pairs were compiled into a histogram (23 cm^{-1} bin width). Vibrations were identified by relying on Colthup, Daly & Wiberley (1990), the ChemCompute + GAMESS quantum chemistry framework (Perri & Weber 2014; Barca et al. 2020), and the NASA Ames PAH IR spectroscopic data base (Boersma et al. 2014; Bauschlicher et al. 2018; Mattioda et al. 2020). Tentatively, the peaks in Fig. 1 can be assigned to various chemical bonds (e.g. $C\equiv C$, $C\equiv N$, $S-H$, $C-O$, $C=O$, $Si-H$). For example, the potential aromatic out of plane (oop) bending $C-H$ vibration may represent the line near 745 cm^{-1} , which is the most prominent maximum,¹ with an underestimated uncertainty

* E-mail: Daniel.Majaess@msvu.ca

© 2025 The Author(s).

Published by Oxford University Press on behalf of Royal Astronomical Society. This is an Open Access article distributed under the terms of the Creative Commons Attribution License (<https://creativecommons.org/licenses/by/4.0/>), which permits unrestricted reuse, distribution, and reproduction in any medium, provided the original work is properly cited.

¹Linearly binned wavelength (rather than wavenumber) would reveal a maximum toward small λ .

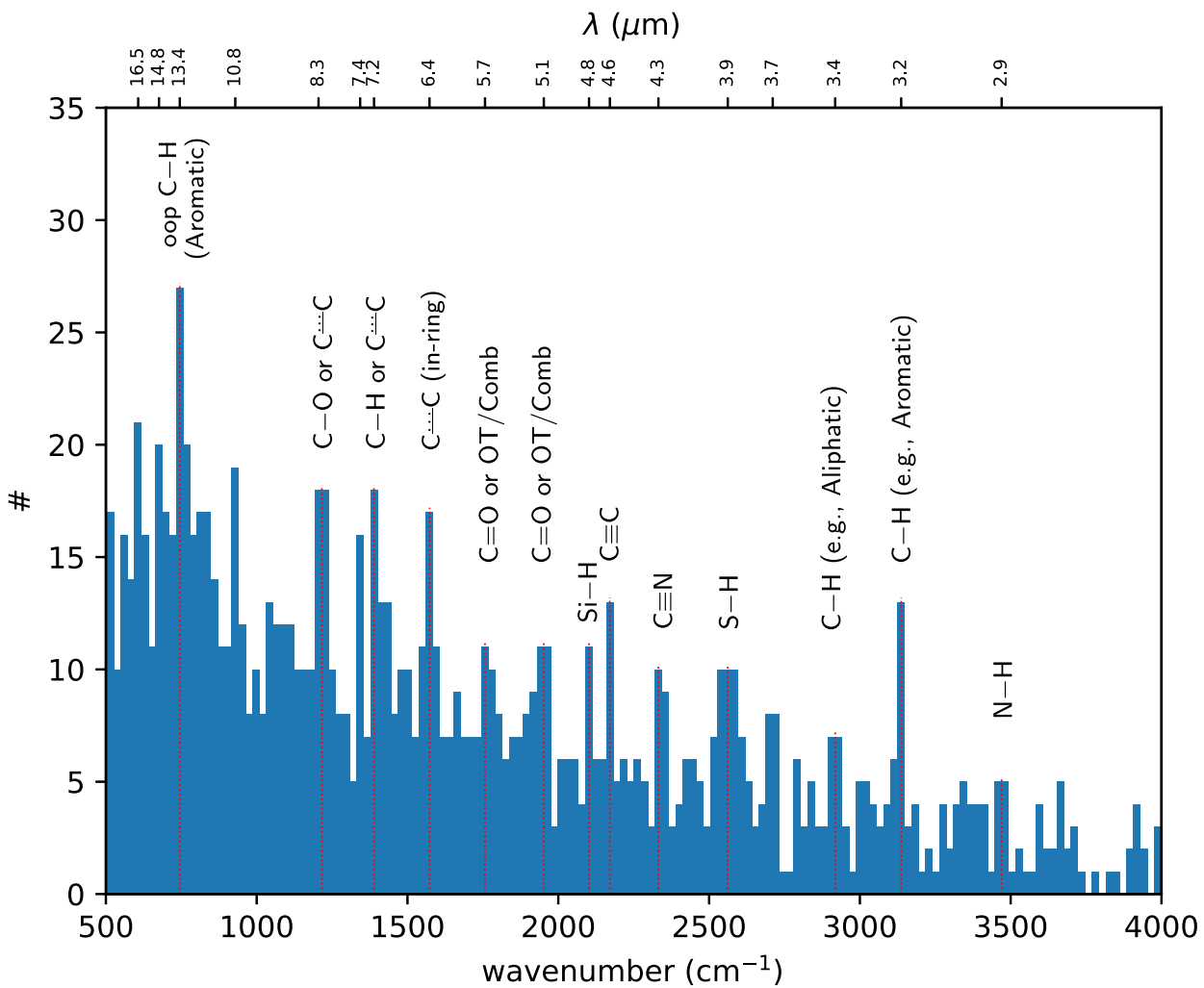


Figure 1. Energy differences between higher correlated DIB pairs ($r - \sigma_r \geq 0.8$, $EW/\sigma_{EW} \geq 5$) may feature histogram maxima that reveal the underlying chemical bonds (tentative candidates are suggested, e.g. the principal $745 \pm 12 \text{ cm}^{-1}$ peak). Degeneracies exist owing to broadening and overlapping wavenumbers. Independent investigations are needed to evaluate the histogram approach and spurious maxima. Data were extracted from the APO DIB catalogue.

(formal) being half the bin width (i.e. $745 \pm 12 \text{ cm}^{-1}$). Peaks in its vicinity could represent differing aromatic substitution patterns. The prominence of $\simeq 745 \text{ cm}^{-1}$ ($13.4 \mu\text{m}$) in concert with $\simeq 697 \text{ cm}^{-1}$ ($14.8 \mu\text{m}$) may be indicative of mono-substitution. The feature near 606 cm^{-1} ($16.5 \mu\text{m}$) was identified by Moutou et al. (2000) as linked to PAHs (see also Bondar 2020, and their DIB family). Aromatics are likewise relayed by the in-ring $C\cdots C$ line perhaps appearing near 1573 cm^{-1} , and $C-H$ line beyond $\simeq 3000 \text{ cm}^{-1}$, while shortward of the latter are aliphatic $C-H$ (or perhaps as an aliphatic group attachment). Furthermore, overdensities near 5.25 (FWHM $\approx 0.12 \mu\text{m}$) and $5.7 \mu\text{m}$ (FWHM $\approx 0.17 \mu\text{m}$) can be conducive to PAH overtones, combinations, etc. (Boersma et al. 2009, and references therein). The two longer wavelength $C\cdots C$ may be tied to fullerenes, and a degeneracy could likewise extend to the putative $10.8 \mu\text{m}$ and oop $C-H$ features. The diversity of vibrational transitions reaffirms prior analyses indicating numerous molecules give rise to DIBs (e.g. on the basis of correlated equivalent widths, common correlations relative to reddening, and spectral line morphology, Cami et al. 1997; Smith et al. 2021, 2022; Ebenbichler et al. 2024).

Crucially, artefacts may exist owing to noise (e.g. $N-H$), and a balance was sought where sufficient statistics were achieved in concert with a reasonable selection of the correlation threshold, sightline number, and binning. Consequently, a histogram for DIB pairs displaying low correlations was constructed (i.e. $|r \pm \sigma_r| \leq 0.5$, Fig. 2) as one possible means of assessing the veracity of the maxima. The maxima were expectedly sensitive to the criteria selected (e.g. $r - \sigma_r \geq 0.8$). The dominant $\simeq 745 \text{ cm}^{-1}$ line that characterized higher correlated DIB pairs (Fig. 1) vanishes, and the underlying substructure at smaller wavenumbers is likewise absent. A subset of vibrational modes potentially remain with less significance owing to the lower correlation criterion, with only one exceeding 3σ . The red dotted lines in Fig. 2 stem from the bin centers of Fig. 1. Sample sizes for Figs 1 and 2 are 1143 and 854 DIB pairs, accordingly.

Yet ultimately, the preliminary vibrations designated in Fig. 1 require further benchmarking and independent vetting. Adjustments shall likewise proceed as a consensus is achieved over time, since vibrational modes can overlap, their wavelengths can shift owing to other constituents within the molecule, and broadening and

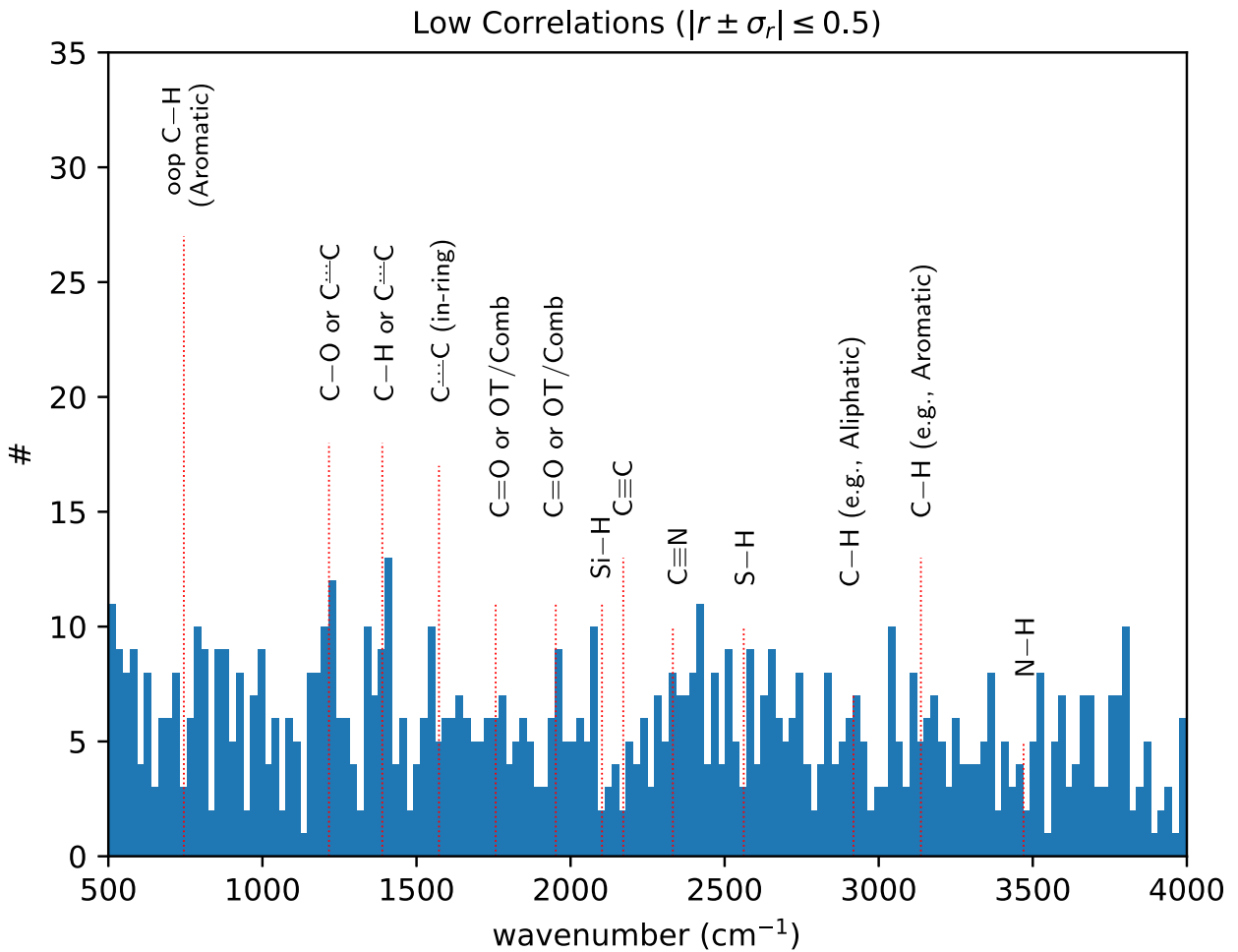


Figure 2. Energy differences between low correlation DIB pairs ($|r \pm \sigma_r| \leq 0.5$). Relative to the high correlation analysis (Fig. 1), the dominant line and substructure at smaller wavenumbers are comparatively absent. Expectedly, a lower significance is apparent for a subset of vibrational modes that possibly remain.

degeneracies occur (e.g. Zapata Trujillo, Pettyjohn & McKemmish 2023).

3 CONCLUSIONS

In this brief exploratory note, DIB energy differences (e.g. Fig. 1) may unveil the building blocks inherent to the broader host molecules. For example, aromatics (e.g. hydrocarbons and potentially heterocycles) and fullerenes could represent a subset of DIB carriers (Fig. 1), as noted previously (e.g. Kroto 1987). Subsequent key steps moving forward include continuing to isolate DIB families (i.e. same carrier) on a multidimensional basis of equivalent widths, optical and near-infrared reddening, line profiles, etc. (e.g. Ebenbichler et al. 2024). Such ongoing research is required to mitigate the noise in Fig. 1, which partly arises from correlated DIB pairs linked to separate carriers whose abundances are commensurate. A critical aspect is to correctly unveil the DIB tied to the origin band, which may represent the transition to the ground vibration of the first excited electronic state². Concurrently, the APO catalogue can be expanded

by extracting additional EWs from high-quality GOSSS and X-shooter spectra (Maíz Apellániz et al. 2013; Verro et al. 2022), while simultaneously characterizing the number and properties of dust clouds along the sightline by utilizing new Gaia DR3 parallax and $\lambda \simeq 330\text{--}1050\,\text{nm}$ spectroscopic observations (Gaia Collaboration 2023; Xing et al. 2024). The latter may provide the desirable rationale behind outliers amongst Pearson correlation determinations (e.g. circumstellar shell for VI Cyg 12, Xing et al. 2024, their fig. 1). Moreover, viewing a DIB through multiple clouds along the sightline can be preferable when establishing broad correlations, thereby mitigating anomalies endemic to any one cloud.

Future work likewise includes awaiting temporally costly extensive vibrational coupled cluster calculations for an expansive set of neutral and cation species, and undertaking analyses of linearly binned wavelength histograms and unidentified infrared emission lines (UIEs).³ DIBs and UIEs should share a subsample of molecules,⁴ however, differences are expected (e.g. λ linked to neutral versus ion species, intensity shifts, separate molecules)

²Slight offsets between observed vibrational wavenumbers implied by DIB pairs relative to those in compilations are expected if the latter are linked to the ground electronic state.

³Kwok (2022) favors mixed aromatic/aliphatic organic nanoparticles (MAONs) for UIEs rather than canonical PAHs.

⁴e.g. Bondar (2020), and for C_{60}^+ see Foing & Ehrenfreund (1994, DIBs) and Sadjadi et al. (2022, UIEs).

owing to disparate ambient temperatures, densities, neutral and ion population ratios, radiation field, etc. (broader discussions in Peeters 2002 and Bondar 2020 and references therein).

ACKNOWLEDGEMENTS

This research relied on initiatives such as the APO DIB catalogue, CDS, NASA ADS, arXiv, NASA Ames PAH IR spectroscopic data base, ChemCompute + GAMESS.

DATA AVAILABILITY

The data underlying this article are readily available via the Centre de Données astronomiques de Strasbourg (CDS), and the Fan et al. (2019) reference.

REFERENCES

- Barca G. M. J. et al., 2020, *The Journal of Chemical Physics*, 152, 154102
 Bauschlicher C. W., Jr, Ricca A., Boersma C., Allamandola L. J., 2018, *ApJS*, 234, 32
 Boersma C., Mattioda A. L., Bauschlicher C. W., Jr, Peeters E., Tielens A. G. G. M., Allamandola L. J., 2009, *ApJ*, 690, 1208
 Boersma C. et al., 2014, *ApJS*, 211, 8
 Bondar A., 2012, *MNRAS*, 423, 725
 Bondar A., 2020, *MNRAS*, 496, 2231
 Cami J., Sonnentrucker P., Ehrenfreund P., Foing B. H., 1997, *A&A*, 326, 822
 Campbell E. K., Holz M., Gerlich D., Maier J. P., 2015, *Nature*, 523, 322
 Colthup N. B., Daly L. H., Wiberley S. E., 1990, in Colthup N. B., Daly L. H., Wiberley S. E., eds, Introduction to Infrared and Raman Spectroscopy (Third Edition), third edition edn, Academic Press, San Diego, p. 387 <http://www.sciencedirect.com/science/article/pii/B9780080917405500168>
 Ebenbichler A. et al., 2024, *A&A*, 686, A50
 Fan H. et al., 2019, *ApJ*, 878, 151
 Foing B. H., Ehrenfreund P., 1994, *Nature*, 369, 296
 Gaia Collaboration, 2023, *A&A*, 674, A1
 Galazutdinov G. A., Shimansky V. V., Bondar A., Valyavin G., Krełowski J., 2017, *MNRAS*, 465, 3956
 Galazutdinov G. A., Valyavin G., Ikhsanov N. R., Krełowski J., 2021, *AJ*, 161, 127
 Hartmann J., 1904, *ApJ*, 19, 268
 Heger M. L., 1922, Lick Observatory Bulletin, 10, 146
 Jenniskens P., Desert F. X., 1993, *A&A*, 274, 465
 Kroto H. W., 1987, Chains and Grains in Interstellar Space. Springer Netherlands, Dordrecht, p. 197, https://doi.org/10.1007/978-94-009-477-4_17
 Kwok S., 2022, *Ap&SS*, 367, 16
 Maíz Apellániz J. et al., 2013, in Massive Stars: From alpha to Omega. p. 198, preprint ([arXiv:1306.6417](https://arxiv.org/abs/1306.6417))
 Majaess D., Harriott T. A., Seuret H., Morera-Boado C., Massa L., Matta C. F., 2025, *MNRAS*, 538, 2392
 Maryeva O. V., Chentsov E. L., Goranskij V. P., Dyachenko V. V., Karpov S. V., Malogolovets E. V., Rastegaev D. A., 2016, *MNRAS*, 458, 491
 Mattioda A. L. et al., 2020, *ApJS*, 251, 22
 McCall B. J. et al., 2010, *ApJ*, 708, 1628
 Moutou C., Krełowski J., D'Hendecourt L., Jamroszczak J., 1999, *A&A*, 351, 680
 Moutou C., Verstraete L., Léger A., Sellgren K., Schmidt W., 2000, *A&A*, 354, L17
 Nie T. P., Xiang F. Y., Li A., 2022, *MNRAS*, 509, 4908
 Omont A., 2016, *A&A*, 590, A52
 Peeters E., 2002, PhD thesis, University of Groningen, Netherlands
 Perri M. J., Weber S. H., 2014, *J. Chemical Edu.*, 91, 2206
 Sadjadi S., Parker Q. A., Hsia C.-H., Zhang Y., 2022, *ApJ*, 934, 75
 Schlarmann L., Foing B., Cami J., Fan H., 2021, *A&A*, 656, L17
 Smith F. M., Harriott T. A., Majaess D., Massa L., Matta C. F., 2021, *MNRAS*, 507, 5236
 Smith E. R., Smith F. M., Harriott T. A., Majaess D., Massa L., Matta C. F., 2022, *RNAAS*, 6, 82
 Verro K. et al., 2022, *A&A*, 660, A34
 Xing H., Sullivan A., Seuret H., Morera-Boado C., Harriott T. A., Majaess D., Massa L., Matta C. F., 2024, *RNAAS*, 8, 90
 Zapata Trujillo J. C., Pettyjohn M. M., McKemmish L. K., 2023, *MNRAS*, 524, 361

This paper has been typeset from a TeX/LaTeX file prepared by the author.